



# Synergic effect of silver nanoparticles and carbon nanotubes on the simultaneous voltammetric determination of hydroquinone, catechol, bisphenol A and phenol

Lorena Athie Goulart<sup>1</sup> · Roger Gonçalves<sup>1</sup> · Alessandra Alves Correa<sup>1</sup> · Ernesto Chaves Pereira<sup>1</sup> · Lucia Helena Mascaro<sup>1</sup>

Received: 10 July 2017 / Accepted: 9 November 2017 / Published online: 5 December 2017

© Springer-Verlag GmbH Austria, part of Springer Nature 2017

## Abstract

A glassy carbon electrode (GCE) was modified with multi-walled carbon nanotubes (MWCNT) and silver nanoparticles (AgNPs) and applied to the simultaneous determination of hydroquinone (HQ), catechol (CC), bisphenol A (BPA) and phenol by using square-wave voltammetry. The MWCNTs were deposited on the GCE and the AgNPs were then electrodeposited onto the MWCNT/GCE by the application of 10 potential sweep cycles using an AgNP colloidal suspension. The modified GCE was characterized by using SEM, which confirmed the presence of the AgNPs. The electrochemical behavior of the material was evaluated by using cyclic voltammetry, and by electrochemical impedance spectroscopy that employed hexacyanoferrate as an electrochemical probe. The results were compared to the performance of the unmodified GCE. The modified electrode has a lower charge-transfer resistance and yields an increased signal. The peaks for HQ (0.30 V), CC (0.40 V), BPA (0.74 V) and phenol (0.83 V; all versus Ag/AgCl) are well separated under optimized conditions, which facilitates their simultaneous determination. The oxidation current increases linearly with the concentrations of HQ, CC, BPA and phenol. Detection limits are in the order of 1  $\mu$ M for all 4 species, and the sensor is highly stable and reproducible. The electrode was successfully employed with the simultaneous determination of HQ, CC, BPA and phenol in spiked tap water samples.

**Keywords** Multi-walled carbon nanotubes · AgNPs · Metallic nanoparticles · Sensor · Phenolic compounds · Voltammetry · Endocrine disruptor · Emerging pollutants · Simultaneous determination · Electrochemical detection

## Introduction

Carbon nanotubes (CNTs) are very versatile and can be applied in different electrochemical devices. They are materials that are structured in the nanometer scale with unique properties, such as high tensile strength and electrical and thermal conductivity [1]. Multi-walled carbon nanotubes (MWCNTs) are widely employed and used to build electrochemical sensors and biosensors due its catalytic properties and high surface area [2].

Acid treatments [3] and the incorporation of metallic nanoparticles [4] within the CNTs are an alternative with which to improve the analytical response of the sensors, thereby resulting in low detection limits [5]. The metallic nanoparticles that are most often used are gold, nickel, copper oxide and silver [6, 7].

Silver nanoparticles (AgNPs) have stood out because they are inexpensive, easy to obtain and offer excellent catalytic properties [8]. Different methods have been reported for the deposition of nanoparticles on CNTs. The most frequently used are casting, spin coating and electrodeposition [9]. The electrochemical procedure presents advantages because of its simplicity and quickness.

In this work, a sensor based on MWCNTs and AgNP was developed for the detection of phenolic compounds such as hydroquinone (HQ), catechol (CC), bisphenol A (BPA) and phenol (Phe). These substances are commonly used in the manufacture of plastic bottles, metal food cans, cosmetics, and pesticides [10]. However, these compounds are emerging

**Electronic supplementary material** The online version of this article (<https://doi.org/10.1007/s00604-017-2540-5>) contains supplementary material, which is available to authorized users.

✉ Lucia Helena Mascaro  
lmascaro@ufscar.br

<sup>1</sup> Department of Chemistry, Universidade Federal de São Carlos, CP 676, São Carlos-SP 13565-905, Brazil

as pollutants because they are not degraded in conventional water treatment processes. Moreover, they can cause harm to the environment and animals. Studies indicate that these phenolic compounds can affect the endocrine system and damage the reproductive system [11]. In addition, exposure to these substances can lead to neurological problems, obesity, diabetes and breast and prostate cancer [12–14].

Due to the low degradability and high toxicity of these compounds in the environment, different analytical methods have been developed for their detection. Among these methods, the electrochemical approach stands out due to its low implementation and running costs, simple operation, high sensitivity and selectivity [15].

The electrochemical detection of HQ, CC, BPA and Phe is usually done individually or in pairs, such as HQ and CC or BPA and Phe, for example [16–25]. This is because the oxidation potencies of these phenolic compounds are very close and are generally difficult to separate into voltammograms. Thus, developing a method capable of selectively detecting a mixture of phenolic compounds has been a major challenge. In this work, we endeavored to develop, for the first time, a modified electrode with MWCNTs and AgNP that is capable of simultaneously determining four phenolic compounds in water samples.

## Experimental

### Reagents

Hydroquinone, catechol, bisphenol A and phenol were purchased from Sigma-Aldrich and used without further purification. MWCNT samples (purity of 95%, length of 5–15  $\mu\text{m}$ , diameter of 20–40 nm) were acquired from Shenzhen Nanotech Port Co., Ltd. – China (<http://www.nanotubes.com.cn/>). Silver nitrate, sodium borohydride and polyvinyl alcohol (PVA) were obtained from Sigma-Aldrich (<http://www.sigmaaldrich.com/>). Sulfuric acid and nitric acid were acquired from Synth (<http://www.labsynth.com.br/>).  $\text{Na}_2\text{HPO}_4$ ,  $\text{Na}_2\text{HPO}_4$ , HCl, NaOH and KCl from Synth. All aqueous solutions were prepared with ultra-purified water from a Millipore Milli-Q system ( $>18.2 \text{ M}\Omega\cdot\text{cm}$ ). Phosphate buffer (PB;  $0.1 \text{ mol}\cdot\text{L}^{-1}$ ) was prepared with  $\text{Na}_2\text{HPO}_4$  and  $\text{Na}_2\text{HPO}_4$  and ultra-purified water. NaOH and HCl solutions ( $0.1 \text{ mol}\cdot\text{L}^{-1}$ ) were used for adjust of pH of the buffer solutions.

### Apparatus

Electrochemical experiments were carried out using an Autolab potentiostat/galvanostat, model PGSTAT30 (Eco Chemie, Utrecht, Netherlands), controlled by the GPES 4.9 software. Electrochemical impedance spectroscopy (EIS) was conducted at open circuit potential (OCP) and Autolab PGSTAT30.

A three-electrode cell was employed for the electrochemical measurements using bare or modified GCE (5.0 mm diameter) as the working electrode. Ag/AgCl ( $\text{KCl } 3.0 \text{ mol}\cdot\text{L}^{-1}$ ) and platinum wire were used as reference and auxiliary electrodes, respectively. Cyclic voltammetry (CV) was used to characterize the sensors and to study the voltammetric behavior of the analytes (BPA, HQ, CC, and Phe). CV measurements were carried out in the potential range from  $-0.3 \text{ V}$  to  $+1.0 \text{ V}$  with a scan rate of  $50 \text{ mV s}^{-1}$ . The EIS experiments scanned a frequency range from 100 kHz to 100 MHz with 10 mV of amplitude. The square wave voltammetry (SWV) technique was used for individual and simultaneous electrochemical detection of BPA, HQ, CC, and Phe. For the SWV measurements, a frequency of 10 Hz, amplitude of 20 mV and a step potential of 2 mV were employed. Analytical curves were obtained from the addition of volumes of standard solutions of HQ, CC, BPA and Phe. The detection limits (LOD) were obtained according to the recommendation from IUPAC [26].

Morphological characterization of the films was made using a scanning electron microscope coupled to a field emission gun (FEG-SEM), (Zeiss model Supra 35) equipped with a secondary high definition detector operating at 6 kV with a resolution of 3.8 nm.

### Synthesis of AgNP

The AgNP were prepared at a temperature of  $4 \text{ }^\circ\text{C}$  to reduce silver nitrate with sodium borohydride, as previously described [27], but with some modifications: 30 mL of a  $0.02 \text{ mmol}\cdot\text{L}^{-1}$  solution of polyvinyl alcohol (PVA) was mixed with 20 mL of a  $4.6 \text{ mmol}\cdot\text{L}^{-1}$  silver nitrate solution and the mixture was stirred for 5 min. Then, 10 mL of sodium borohydride  $0.53 \text{ mmol}\cdot\text{L}^{-1}$  was added to the reactional medium. After that, the solution turned light yellow, thus confirming the formation of AgNP. After this, the solutions were stored in dark bottles in the refrigerator. No further purification was performed.

### Preparation of AgNP/MWCNT/GCE

First, the MWCNTs were pre-treated using a solution of concentrated sulfuric and nitric acids in the proportion of 3:1 v/v, respectively. The mixture was stirred for 12 h at room temperature and the filtration and washing processes were subsequently carried out. Then, the nanotubes were dried in an oven for 12 h at  $70 \text{ }^\circ\text{C}$  [28]. It is known that the pre-treatment of CNT can lead to the enhancement of its catalytic properties. In this process occur changes of morphology, unblocking of the ends of the CNT, a sharp decrease in the diameter of the tubes, an increase of superficial area. Besides, there are the effective incorporation of different functional groups such as epoxide, hydroxyl, carboxyl and other oxygenated species [29]. After the pretreatment, 1.0 mg of MWCNTs was added to 1.0 mL of

dimethylformamide (DMF) and this suspension was stirred in ultrasonic bath for 30 min.

The AgNP/MWCNT/GCE was prepared as follows: an aliquot of 10  $\mu\text{L}$  of the MWCNTs suspension in DMF was placed as a droplet on the bare GCE. The solvent is evaporated at the room temperature to form the MWCNT/GCE. The incorporation of AgNP at the MWCNTs film was pre-optimized and was carried out using CV (10 scans between  $-0.2$  V and  $0.4$  V at a scan rate of  $100$   $\text{mV s}^{-1}$ ) in  $22$  mL of a  $0.1$   $\text{mol.L}^{-1}$  KCl solution containing  $3.0$  mL of AgNP solution [30]. After this, the AgNP/MWCNT/GCE sensor was obtained (Scheme 1).

## Analytical application

Tap water samples were collected at the University Federal of São Carlos, SP, Brazil, at the Laboratório Interdisciplinar de Eletroquímica e Cerâmica (LIEC) in the chemistry department. The tap water samples were not treated in any way. To obtain electrochemical measurements,  $5$  mL of the tap water samples were added to a  $10$ -mL volumetric flask and the volume was filled up with phosphate buffer with a pH of 3. In the addition and recovery study, the water samples were fortified at concentrations of  $10$  and  $30$   $\text{mg.L}^{-1}$  of HQ, CC, BPA and Phe. Aliquots of the standard solution of HQ, CC, BPA and Phe ( $1.0 \times 10^{-3}$   $\text{mol.L}^{-1}$ ) were added to  $10$  mL of fortified water samples for the construction of the analytical curves. SWV was the technique that was used for the electrochemical detection of BPA, HQ, CC, and Phe. The potentials of oxidation that were used to obtain the current peak were  $+0.28$  V for HQ,  $+0.39$  V for CC,  $+0.72$  V for BPA and  $+0.82$  V for Phe. The analyte concentrations in the water sample were calculated by applying the extrapolation method.

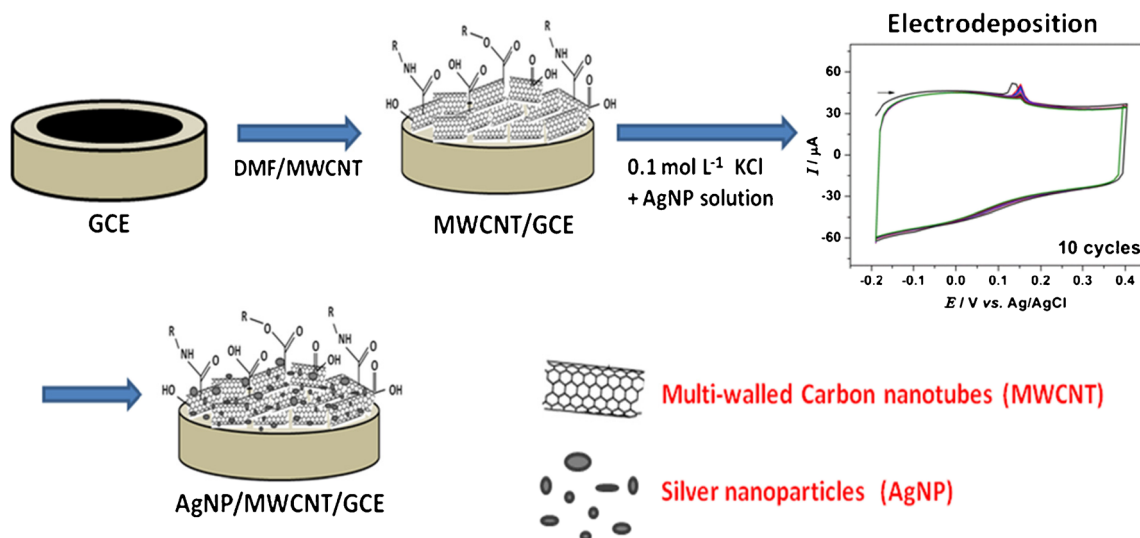
## Results and discussion

### Choice of materials

MWCNTs present a high surface area, excellent electrical and thermal conductivity and can promote electronic interaction with electroactive molecules and electrochemical sensors. After acid treatments, there is a significant improvement in the catalytic properties of MWCNTs. This is related to the increase of the surface area, besides the addition of functional groups in its structure. In addition, MWCNTs form stable and reproducible films when deposited on glassy carbon substrates. These characteristics make it an excellent candidate in the manufacture of electrochemical sensors. The stability of the film is also attributed to the solvent used in dispersing MWCNTs. DMF was used because, with it the MWCNTs forms a more homogeneous film than other solvents, such as ethanol and acetone. To increase the conductivity of the carbon films, AgNP were electrodeposited. AgNP were chosen because of their excellent conductivity, fast synthesis and low cost. Moreover, they have a synergistic effect with carbon materials, leading to the formation of a very catalytic material. The electrodeposition of the nanoparticles was chosen as the deposition technique due to its simplicity.

### Morphology and composition of AgNP/MWCNT film

The morphological characterization of the MWCNTs and AgNP/MWCNT films were performed by SEM and the results are presented in Fig. 1. The MWCNTs were uniformly distributed over the GCE surface, as can be observed in Fig. 1a. After the electrodeposition step, white dots, which indicate the presence of metallic particles, were observed over the MWCNTs on the surface of the material, Fig. 1b. To facilitate the observation



**Scheme 1** Schematic diagram for the sensor manufacture (AgNP/MWCNT/GCE)

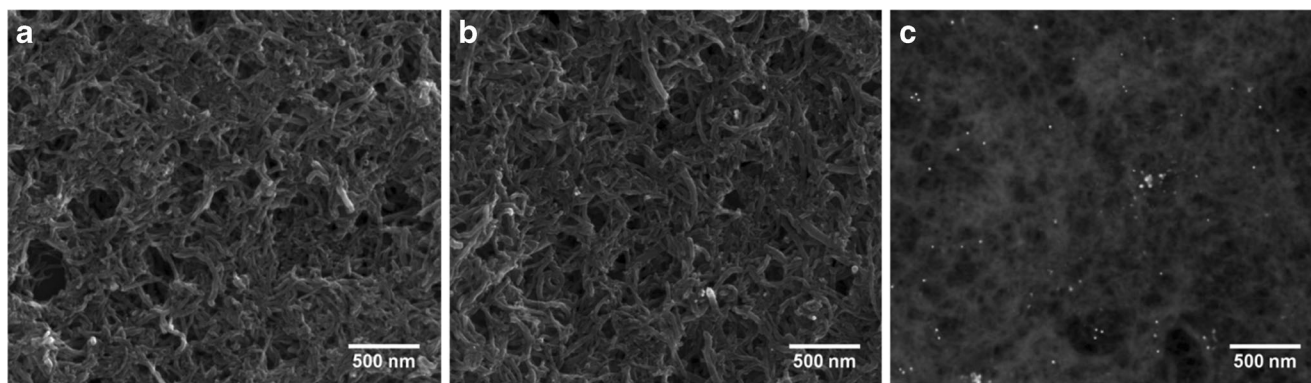


**Fig. 1** SEM images of MWCNTs (a) AgNP/MWCNT (b) and AgNP/MWCNT obtained in the backscatter mode (c)

of AgNP, the SEM backscattered mode was used, Fig. 1c. The AgNP average size is 32 nm. To stress the presence of AgNP, an energy-dispersive X-ray spectroscopy (EDS) analysis was performed; the results are presented in Fig. S1 in Supplementary Material. The method of electrodepositing of AgNP on MWCNTs was chosen because it is quick. In addition, it is possible to control the thickness of the deposited layer [51].

### Electrochemical characterization of AgNP/MWCNT/GCE

The electrochemical deposition of the AgNP at the sensors was confirmed by CV (Fig. S2-Supplementary Material). In the cyclic voltammogram of the AgNP/GCE electrode a well defined redox pair was observed at  $-0.07$  V and  $+0.14$  V associated with  $\text{Ag}^+/\text{Ag}^0$  conversion. Similar voltammograms

of AgNP were previously described [31]. The presence of AgNP in the MWCNTs film is confirmed by the typical oxidation peak of the nanoparticles in  $+0.14$  V. In the cyclic voltammogram of the AgNP/MWCNT/GCE, two oxidation and reduction processes in  $+0.3$  V and  $0.2$  V appear. These processes may be related to the oxidant species present in the MWCNTs after their functionalization and may have masked the peak of reduction of AgNP. The electro catalytic effect of the AgNP/MWCNT/GCE was evaluated through CV and EIS. Figure 2 shows the cyclic voltammograms and the Nyquist plots for GCE, AgNP/GCE, MWCNT/GCE and AgNP/MWCNT/GCE in the presence of  $5.0 \text{ mmol.L}^{-1}$  of ferricyanide in  $0.1 \text{ mol.L}^{-1}$  KCl. The voltammograms show the response of the electrode and an increase of current is noticeable for the samples modified with MWCNTs and MWCNTs decorated with AgNP. The stability of the nanoparticles in the medium

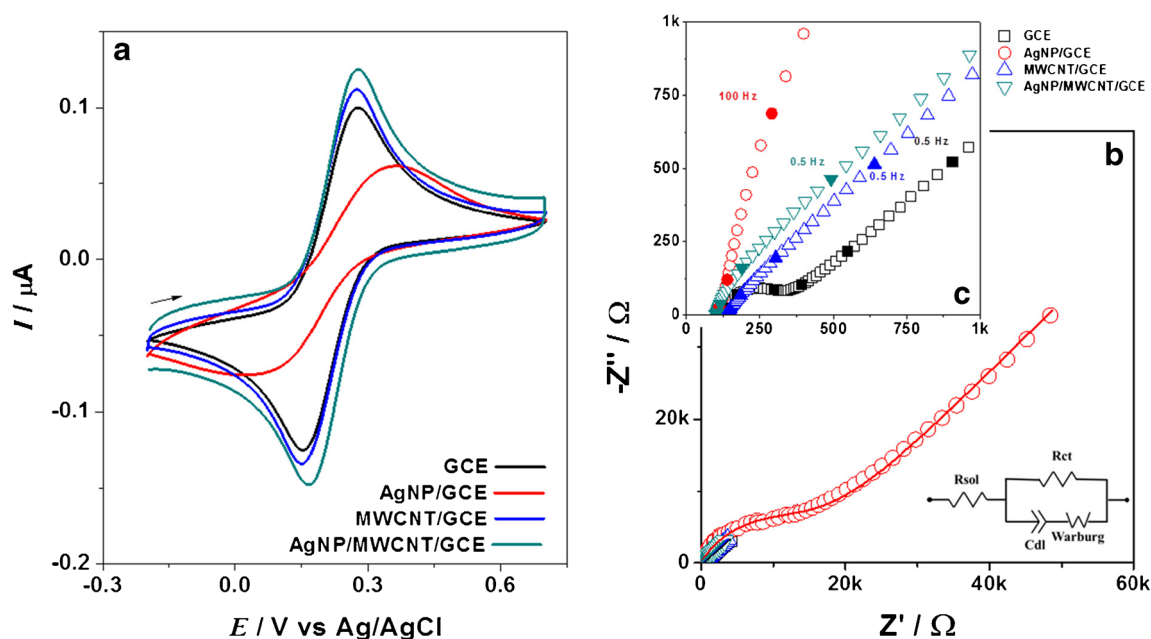


**Fig. 2** CVs (a) and Nyquist plot (b) zoom of Nyquist plot (c) obtained in presence of  $5.0 \text{ mmol.L}^{-1}$  of  $\text{Fe}^{2+}/\text{Fe}^{3+}$  redox pair in  $0.1 \text{ mmol.L}^{-1}$   $\text{H}_2\text{SO}_4$ . EIS performed at the oxidation peak potential, from 10 kHz down to 100 MHz with 10 mV of amplitude

was observed by means of CV before and after immersion and cycling of the electrode in ferricyanide medium. It was observed no change between one voltammetric profile and another, attesting that the nanoparticles are not affected.

The EIS data was fitted by using an equivalent circuit and Table S1 (supplementary material) summarizes the values that were obtained for the oxidation of the  $\text{Fe}^{2+}/\text{Fe}^{3+}$  redox pair. It is possible to verify that, when the AgNPs are deposited over the GCE, they lead to a less effective electrode response. This result is attributed to the slow electronic transfer between these two materials. On the other hand, when the AgNPs are deposited on the MWCNT, the nanoparticles cause a decrease in the charge transfer resistance (from  $236 \Omega$  to  $116 \Omega$ ), in addition to a small increase in the electrochemical area (from  $49.1 \mu\text{F s}^{-1}$  to  $51.7 \mu\text{F s}^{-1}$ ). Additionally, the deposition of AgNPs on the nanotubes produced a surprising result; the estimated charge transfer rate ( $8.3 \times 10^4 \text{ s}^{-1}$ ) is approximately twice those verified for both GCE and MWCNTs ( $3.4 \times 10^4 \text{ s}^{-1}$  and  $4.3 \times 10^4 \text{ s}^{-1}$ , respectively). Thus, the rate with which the charge is transferred is two times higher, due to the presence of the nanoparticles. These results support the idea that there is a synergism between AgNPs and MWNTCs. This can be explained by the higher rate of charge transfer that occurs between both AgNP and analyte and then AgNP and MWCNTs. While the rate of charge transfer is not so high between the GCE and the nanoparticles, there is thus a decrease in the electrocatalytic activity of GCE decorated with AgNP.

### Electrochemical behavior of HQ, CC, BPA and Phe

Figure 3 shows the schematic diagram with CV responses of a mixture of the studied species (HQ, CC, BPA and Phe) in a potential range from  $-0.2 \text{ V}$  to  $+1.0 \text{ V}$  in PB of pH 6.0 over the different electrodes. Two broad oxidation and reduction peaks with low resolution and intensity were observed on the bare GCE, Fig. 3a. This behavior indicates that the molecules under study cannot be distinguished on the bare electrode. A similar behavior was observed in the CV obtained by using the AgNP/GCE sensor, Fig. 3b. The characteristic oxidation peak of AgNP was observed in the voltammogram in PB. However, with the oxidation of the phenolic compounds, the peak was not observed in the cyclic voltammogram. This behavior may indicate the low adhesion of the nanoparticles to the surface of the CGE since there was no improvement in the resolution of phenol oxidation peaks. However, the GCE modified with MWCNTs promoted the separation of the peaks related to the oxidation of the species, Fig. 3c. The current peak potentials are  $+0.15 \text{ V}$ ,  $+0.25 \text{ V}$ ,  $+0.59 \text{ V}$  and  $+0.67 \text{ V}$  for HQ, CC, BPA and Phe, respectively. The same oxidation peak potentials were observed for AgNP/MWCNT/GCE and, in addition, the current peak was more intense, Fig. 3d. The AgNP peak appears on the cyclic voltammogram, along with the hydroquinone oxidation peak at a pH of 6.0.

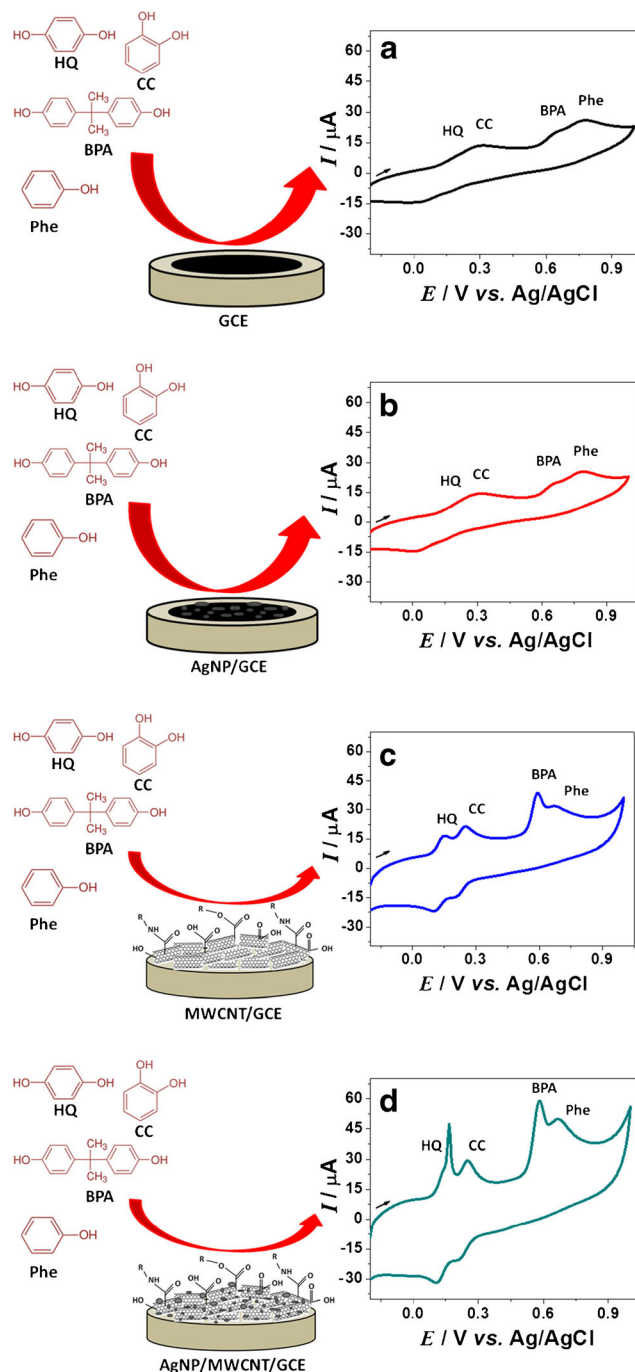


**Fig. 3** Schematic diagrams of the electro-oxidation of  $1.0 \times 10^{-4} \text{ mol.L}^{-1}$  of HQ, CC, BPA and Phe with cyclic voltammogram recorded at the bare GCE (a), AgNP/CGE (b), MWCNT/GCE (c) and AgNP/MWCNT/GCE (d) at a scan rate of  $50 \text{ mV s}^{-1}$  in  $0.1 \text{ mol.L}^{-1}$  phosphate buffer of pH 6.0

However, at a pH of 3.0, which is the optimized condition, the oxidation peaks of Ag and HQ do not overlap.

The results indicate that the AgNP under the MWCNTs film can accelerate electron transfer, as suggested by the electrochemical impedance data. The simultaneous detection of the four species is possible because each species oxidizes at a different potential on the surface of the modified electrode

with MWCNTs and AgNP. This is due to the faster charge transfer; there is a narrowing of the peaks, leading to a better separation these peaks and an increase in the selectivity of the electrode among the different analytes. This is not observed in the GCE electrode, for example, which presents a smaller surface area in comparison to the AgNP/MWCNT/GCE electrode. The oxidation processes that leads to a voltammogram peaks very close as HQ and CC and of BPA and Phe, is possible to observe no separation of these peaks in the bare GCE. The oxidation mechanisms of the studied species are presented in the Supplementary Material, Fig. S3.

### Optimization of method

To improve the analytical response of the sensor, some parameters have been studied: (a) the effect of pH; (b) the effect of the scan rate and (c) the parameters of the SWV technique. The [Electronic Supporting Material](#) section presents the respective data and figures. The following experimental conditions were found to give the best results: (a) a sample pH value of 3.0; (b) a linear relationship between the peak current and the square root of the scan rate ( $v^{1/2}$ ) was obtained from 5 to 100  $\text{mV}\cdot\text{s}^{-1}$  for HQ, CC and Phe. It is also observed a linear relationship between the peak current and the scan rate ( $v$ ) for BPA; (c) frequency of 10 Hz, amplitude of 20 mV and step potential of 2 mV to SWV.

### Individual and simultaneous determination of HQ, CC, BPA and Phe

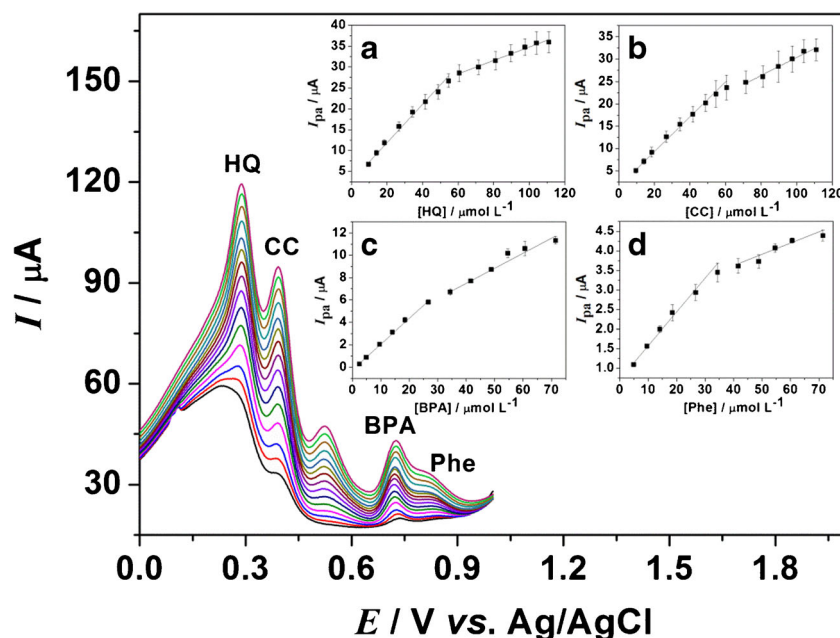
The AgNP/MWCNT/GCE sensor was used in the separate and simultaneous determination of HQ, CC, BPA and Phe using the SWV technique. Initially, separated determinations

for each substance were made by changing its concentration and keeping all other concentrations constant. The anodic peaks current for HQ, CC, BPA and Phe were obtained at a working voltage of +0.28 V to HQ, +0.39 V to CC, +0.72 V to BPA and +0.82 V to Phe (vs. Ag/AgCl) respectively, with scan rate of 20  $\text{mV}\cdot\text{s}^{-1}$ . Fig. S9 (Supplementary Material) shows the square wave voltammograms for different concentrations of HQ at PB of pH 3.0 and 50  $\mu\text{mol}\cdot\text{L}^{-1}$  CC, BPA and Phe. The inset in Fig. S6A is the analytical curve of  $I_{\text{pa}}$  average values vs. the concentration of HQ. The  $I_{\text{pa}}$  was directly proportional to the concentration of HQ in two concentration ranges. The first linear range was from 2.5–56  $\mu\text{mol}\cdot\text{L}^{-1}$  ( $r=0.999$ ) and the second linear range was from 65 to 160  $\mu\text{mol}\cdot\text{L}^{-1}$  ( $r=0.997$ ) with a LOD of 1.2  $\mu\text{mol}\cdot\text{L}^{-1}$  ( $S/N=3$ ), an average of the values obtained from the above two linear ranges.

The SWVs for different concentrations of CC keeping the concentration of HQ, BPA and Phe constant at 50  $\mu\text{mol}\cdot\text{L}^{-1}$  are shown in Fig. 6B. As shown in the inset of Fig. S6B, the  $I_{\text{pa}}$  is proportional to the CC concentration in a range from 19.0–100.0  $\mu\text{mol}\cdot\text{L}^{-1}$  ( $r=0.997$ ) and in a range from 120.0–260.0  $\mu\text{mol}\cdot\text{L}^{-1}$  ( $r=0.997$ ). LOD was 1.6  $\mu\text{mol}\cdot\text{L}^{-1}$  ( $S/N=3$ ). Fig. S6C and Fig. S6D illustrate the same behavior for BPA and Phe, respectively. Two linear ranges were also observed from 4.9–740.0  $\mu\text{mol}\cdot\text{L}^{-1}$  and 82.0–150.0  $\mu\text{mol}\cdot\text{L}^{-1}$  for BPA and 2.6–56.0  $\mu\text{mol}\cdot\text{L}^{-1}$  and 65.0–160.0  $\mu\text{mol}\cdot\text{L}^{-1}$  for Phe. LODs were 2.4  $\mu\text{mol}\cdot\text{L}^{-1}$  for BPA and 3.1  $\mu\text{mol}\cdot\text{L}^{-1}$  for Phe.

The simultaneous determination of HQ, CC, BPA and Phe by AgNP/MWCNT/GCE sensor was made by changing the concentrations of these species simultaneously. In Fig. 4 it is possible to observe that the oxidation peaks of HQ, CC, BPA

**Fig. 4** SWVs obtained in phosphate buffer of pH 3.0 using the AgNP/MWCNT/GCE in the presence of different concentrations of HQ, CC, BPA and Phe. Inset: calibration plots for (a) various concentrations of HQ (9.6–110  $\mu\text{mol}\cdot\text{L}^{-1}$ ), (b) various concentrations of CC (9.6–110  $\mu\text{mol}\cdot\text{L}^{-1}$ ), (c) various concentrations of BPA (2.4–71  $\mu\text{mol}\cdot\text{L}^{-1}$ ) and (d) various concentrations of Phe (5.0–71.0  $\mu\text{mol}\cdot\text{L}^{-1}$ )



and Phe are well separated. Table S4 in Supplementary Material, presents the regression parameters and detection limits of the species studied.

In both individual and simultaneous detection, two linear concentration ranges were observed. By comparing the sensitivities of the analytical curves (slope) in the two linear ranges for each species studied (Table S5 in Supplementary material), it is evident that there is a decrease in the sensitivity in the second range. This may be related to the limitation of electron transfer kinetics between the analytes and the sensor surface [32].

An unexpected current peak appeared at +0.52 V. Fig. S10 in Supplementary Material presents the voltammeteries that were obtained by changing the vertex potential during the anodic scan to investigate this issue. It was found that this peak appears after the vertex reaches the BPA and Phe oxidation potentials. Additionally, voltammeteries were separately performed for each species and are presented in Fig. S11 in Supplementary Material. In this case, it was observed that only in the presence of BPA and Phe is this peak is present in the voltammogram. Therefore, this peak should be related to the formation of BPA and Phe oxidation intermediates. In the literature [33–35] it was found that both have intermediates in common, thus supporting our proposal.

Good sensitivity was observed in the individual and simultaneous determination of HQ, CC, BPA and Phe. The detection limits achieved in this study were in the order of  $10^{-6}$  mol.L<sup>-1</sup>.

The analytical performance of the AgNP/MWCNT/GCE sensor was compared with those of other sensors reported in previous studies, Table 1. Although the LOD values are 2 to 3-fold greater than most limits reported in the literature [16, 17, 20–25], it was possible to simultaneously determine the four molecules — HQ, CC, BPA and Phe — for the first time. This result can be attributed to the synergistic effect between the MWCNTs and AgNPs. The excellent conductivity of MWCNTs and the

electrocatalytic activity of AgNPs may be the main contribution to the separate oxidative processes of the studied molecules, which makes it easy to simultaneously determine them.

## Reproducibility and stability

The reproducibility of the AgNP/MWCNT/GCE sensor was verified by detection of  $1.0 \times 10^{-4}$  mol.L<sup>-1</sup> HQ, CC, BPA and Phe in solution of pH 3.0 using five sensors built on different days. The relative standard deviation (RSD) was 3.8%, 2.6%, 0.8% and 2.3% for HQ, DC, BPA and Phe, respectively, showing that the sensor has a good reproducibility. The stability of the sensor was studied through voltammetric responses after 4 weeks. The sensors were stored in a desiccator at room temperature and under light, without light and in a refrigerator at 4 °C. After 4 weeks, the peak currents were retained under all conditions studied (99.7%, 95.4%, 98.3% and 98.7% for HQ, CC, BPA and Phe respectively). Therefore, the AgNP/MWCNT/GCE sensor showed excellent reproducibility and long-term stability.

## Practical application

To investigate the performance and applicability of the AgNP/MWCNT/GCE sensor for the simultaneous determination of HQ, CC, BPA and Phe, local tap water samples were tested. Since the electroanalytical signals of HQ, CC, BPA and Phe were not observed in the real samples, spike and recovery experiments were carried out by measuring the SWV responses to the samples in which known quantities of species were added. Then, the concentrations of species in the tap water sample were determined through the calibration method; the results are listed in Table S6 in Supplementary Material. The recoveries were 100–101%, 103–104%, 99.1–

**Table 1** Comparison of the new sensor for detection of HQ, CC, BPA and phenol (Phe) with others

Sensor	Method	Linear range (μM)				LOD (μM)				Ref.
		HQ	CC	BPA	Phe	HQ	CC	BPA	Phe	
(MWCNT)/ (DTDAB)/(Ti)		–	2.0–15	–	1.5–25	–	3.1	–	2.9	[16]
BDD	DPV	8–10,000	–	–	50–10,000	1.6	–	–	1.8	[17]
MWNTs/GCE	LSV	2–100	2–100	–	–	0.6	0.6	–	–	[18]
MWNTs/MA	Amperometry	1–100	1–100	–	–	0.3	0.2	–	–	[19]
PANI/MnO <sub>2</sub>	DPV	0.2–100	0.2–100	–	–	0.13	0.16	–	–	[20]
Au-G/GCE	DPV	1–100	1–100	–	–	0.2	0.15	–	–	[21]
ZnS/NiS@ZnS/L-Cys/AuNPs/ GCEs	DPV	0.1–300	0.5–400	–	–	0.024	0.07	–	–	[22]
PME/GR-CPE	Amperometry	7–1000	–	9–1000	–	0.074	–	0.01	–	[23]
SiO <sub>2</sub> /GO/AgNP	DPV	–	–	0.1–2.6	–	–	–	0.004	–	[24]
Pd@TiO <sub>2</sub> –SiC/GCE	DPV	0.01–200	–	0.01–200	–	0.005	–	0.004	–	[25]
AgNP/MWCNT/GCE	SWV	2.5–260	20–260	5.0–152	2.4–152	0.16	0.2	2.4	3.0	This work

99.6% and 95.2–101% for HQ, CC, BPA and Phe, respectively. The results suggested that the AgNP/MWCNT/GCE sensor can be applied to simultaneously determine these species in water samples.

## Conclusions

An electrochemical GCE sensor that was modified with MWCNT and AgNP films was successfully synthesized in this work. The SWV was used to simultaneously determine four phenolic compounds (HQ, CC, BPA and Phe) in water samples. The results showed that the sensor present a good linear range and high stability and reproducibility. To extend the application of the sensor, it is necessary to research the quantification the molecules of interest in the presence of other phenolic compounds in our future work.

**Acknowledgements** The authors gratefully acknowledge #2012/20926-2 and #2013/07296-2 São Paulo Research Foundation (FAPESP), CNPq and CAPES for the financial support.

**Compliance with ethical standards** The author(s) declare that they have no competing interests.

## References

- Ummethala R, Wenger D, Tedde SF et al (2016) Effect of substrate material on the growth and field emission characteristics of large-area carbon nanotube forests. *J Appl Phys* 119:44302. <https://doi.org/10.1063/1.4940418>
- Gooding JJ (2005) Nanostructuring electrodes with carbon nanotubes: a review on electrochemistry and applications for sensing. *Electrochim Acta* 50:3049–3060. <https://doi.org/10.1016/j.electacta.2004.08.052>
- Moraes FC, Cabral MF, Mascaro LH, Machado SAS (2011) The electrochemical effect of acid functionalisation of carbon nanotubes to be used in sensors development. *Surf Sci* 605:435–440. <https://doi.org/10.1016/j.susc.2010.11.014>
- Goulart LA, Mascaro LH (2016) GC electrode modified with carbon nanotubes and NiO for the simultaneous determination of bisphenol A, hydroquinone and catechol. *Electrochim Acta*. <https://doi.org/10.1016/j.electacta.2016.02.174>
- Zeng S, Yong K-T, Roy I et al (2011) A review on functionalized gold nanoparticles for biosensing applications. *Plasmonics* 6:491–506. <https://doi.org/10.1007/s11468-011-9228-1>
- Darvishi S, Karmizadeh F, Kharaziha M (2015) A facile one-step electrochemical synthesis of nickel nanoparticle/Graphene composites for non-enzymatic biosensor applications. *Procedia Mater Sci* 11:142–146. <https://doi.org/10.1016/j.mspro.2015.11.006>
- Jiang L, Gu S, Ding Y et al (2014) Facile and novel electrochemical preparation of a graphene–transition metal oxide nanocomposite for ultrasensitive electrochemical sensing of acetaminophen and phenacetin. *Nano* 6:207–214. <https://doi.org/10.1039/C3NR03620K>
- Nantaphol S, Chailapakul O, Siangproh W (2015) Sensitive and selective electrochemical sensor using silver nanoparticles modified glassy carbon electrode for determination of cholesterol in bovine serum. *Sensors Actuators B Chem* 207:193–198. <https://doi.org/10.1016/j.snb.2014.10.041>
- Pagnanelli F, Altimari P, Bellagamba M et al (2015) Pulsed electro-deposition of cobalt nanoparticles on copper: influence of the operating parameters on size distribution and morphology. *Electrochim Acta* 155:228–235. <https://doi.org/10.1016/j.electacta.2014.12.112>
- Ingerslev F, Vaclavik E, Halling-Sørensen B (2003) Pharmaceuticals and personal care products - a source of endocrine disruption in the environment? *Pure Appl Chem*. <https://doi.org/10.1351/pac200375111881>
- Maffini MV, Rubin BS, Sonnenschein C, Soto AM (2006) Endocrine disruptors and reproductive health: the case of bisphenol-A. *Mol Cell Endocrinol* 254–255:179–186. <https://doi.org/10.1016/j.mce.2006.04.033>
- Garoma T, Matsumoto SA, Wu Y, Klinger R (2010) Removal of bisphenol A and its reaction-intermediates from aqueous solution by ozonation. *Ozone Sci Eng* 32:338–343. <https://doi.org/10.1080/01919512.2010.508484>
- Lin T-M, Lee S-S, Lai C-S, Lin S-D (2006) Phenol burn. *Burns* 32: 517–521. <https://doi.org/10.1016/j.burns.2005.12.016>
- Flickinger CW (1976) The benzenediols: catechol, resorcinol and hydroquinone — a review of the industrial toxicology and current industrial exposure limits. *Am Ind Hyg Assoc J* 37:596–606. <https://doi.org/10.1080/0002889768507526>
- Bakker E (2004) Electrochemical sensors. *Anal Chem* 76:3285–3298. <https://doi.org/10.1021/ac049580z>
- Hashemnia S, Khayatzadeh S, Hashemnia M (2012) Electrochemical detection of phenolic compounds using composite film of multiwall carbon nanotube/surfactant/tyrosinase on a carbon paste electrode. *J Solid State Electrochem* 16:473–479. <https://doi.org/10.1007/s10008-011-1355-2>
- Zhao G-H, Tang Y-T, Liu M-C et al (2007) Direct and simultaneous determination of phenol, hydroquinone and nitrophenol at boron-doped diamond film electrode. *Chin J Chem* 25:1445–1450. <https://doi.org/10.1002/cjoc.200790267>
- Ding Y-P, Liu W-L, Q-S W, Wang X-G (2005) Direct simultaneous determination of dihydroxybenzene isomers at C-nanotube-modified electrodes by derivative voltammetry. *J Electroanal Chem* 575:275–280. <https://doi.org/10.1016/j.jelechem.2004.09.020>
- Zhang D, Peng Y, Qi H et al (2009) Application of multielectrode array modified with carbon nanotubes to simultaneous amperometric determination of dihydroxybenzene isomers. *Sensors Actuators B Chem* 136:113–121. <https://doi.org/10.1016/j.snb.2008.11.010>
- Anu Prathap MU, Satpati B, Srivastava R (2013) Facile preparation of polyaniline/MnO<sub>2</sub> nanofibers and its electrochemical application in the simultaneous determination of catechol, hydroquinone, and resorcinol. *Sensors Actuators B Chem* 186:67–77. <https://doi.org/10.1016/j.snb.2013.05.076>
- Ma X, Liu Z, Qiu C et al (2013) Simultaneous determination of hydroquinone and catechol based on glassy carbon electrode modified with gold-graphene nanocomposite. *Microchim Acta* 180: 461–468. <https://doi.org/10.1007/s00604-013-0949-z>
- Wang Y, Qu J, Li S et al (2015) Simultaneous determination of hydroquinone and catechol using a glassy carbon electrode modified with gold nanoparticles, ZnS/NiS@ZnS quantum dots and L-cysteine. *Microchim Acta* 182:2277–2283. <https://doi.org/10.1007/s00604-015-1568-7>
- Peng J, Feng Y, Han X-X, Gao Z-N (2016) Simultaneous determination of bisphenol A and hydroquinone using a poly(melamine) coated graphene doped carbon paste electrode. *Microchim Acta* 183:2289–2296. <https://doi.org/10.1007/s00604-016-1865-9>
- Campos AM, Raymundo-Pereira PA, Cincotto FH et al (2016) Sensitive determination of the endocrine disruptor bisphenol A at ultrathin film based on nanostructured hybrid material SiO<sub>2</sub>/GO/AgNP. *J Solid State Electrochem* 20:2503–2507. <https://doi.org/10.1007/s10008-015-3098-y>



25. Yang L, Zhao H, Fan S et al (2014) A highly sensitive electrochemical sensor for simultaneous determination of hydroquinone and bisphenol A based on the ultrafine Pd nanoparticle@TiO<sub>2</sub> functionalized SiC. *Anal Chim Acta* 852:28–36. <https://doi.org/10.1016/j.aca.2014.08.037>
26. Committee AM (1987) Recommendations for the definition, estimation and use of the detection limit. *Analyst* 112:199. <https://doi.org/10.1039/an9871200199>
27. de Moura MR, Mattoso LHC, Zucolotto V (2012) Development of cellulose-based bactericidal nanocomposites containing silver nanoparticles and their use as active food packaging. *J Food Eng* 109:520–524. <https://doi.org/10.1016/j.jfoodeng.2011.10.030>
28. Goulart LA, de Moraes FC, Mascaro LH (2016) Influence of the different carbon nanotubes on the development of electrochemical sensors for bisphenol A. *Mater Sci Eng C* 58:768–773. <https://doi.org/10.1016/j.msec.2015.09.073>
29. Balasubramanian K, Burghard M (2005) Chemically functionalized carbon nanotubes. *Small* 1:180–192. <https://doi.org/10.1002/sml.200400118>
30. Rawal R, Chawla S, Pundir CS (2011) Polyphenol biosensor based on laccase immobilized onto silver nanoparticles/multiwalled carbon nanotube/polyaniline gold electrode. *Anal Biochem* 419:196–204. <https://doi.org/10.1016/j.ab.2011.07.028>
31. Van der Horst C, Silwana B, Iwuoha E, Somerset V (2015) Synthesis and characterization of bismuth-silver nanoparticles for electrochemical sensor applications. *Anal Lett* 48:1311–1332. <https://doi.org/10.1080/00032719.2014.979357>
32. Nasirizadeh N, Ghaani M, Shekari Z, Shateri-Khalilabad M (2016) Novel non enzymatic TBHQ modified electrochemical sensor for hydrogen peroxide determination in different beverage samples. *J Braz Chem Soc*. <https://doi.org/10.5935/0103-5053.20160037>
33. Negash N, Alemu H, Tessema M (2014) Flow injection amperometric determination of phenol and Chlorophenols at Single Wall carbon nanotube modified glassy carbon electrode. *Am J Anal Chem* 5:188–198. <https://doi.org/10.4236/ajac.2014.53023>
34. Kolvenbach B, Schlaich N, Raoui Z et al (2007) Degradation pathway of bisphenol A: does ipso substitution apply to phenols containing a quaternary -carbon structure in the para position? *Appl Environ Microbiol* 73:4776–4784. <https://doi.org/10.1128/AEM.00329-07>
35. Hu Z, Leung C-F, Tsang Y-K et al (2011) A recyclable polymer-supported ruthenium catalyst for the oxidative degradation of bisphenol A in water using hydrogen peroxide. *New J Chem* 35: 149–155. <https://doi.org/10.1039/C0NJ00583E>